

# Ultrasonic monitoring of early-stage biofilm growth on polymeric surfaces

Elmira Kujundzic<sup>a</sup>, A. Cristina Fonseca<sup>b</sup>, Emily A. Evans<sup>b</sup>, Michael Peterson<sup>c</sup>,  
Alan R. Greenberg<sup>a</sup>, Mark Hernandez<sup>b,\*</sup>

<sup>a</sup> Department of Mechanical Engineering, Membrane Applied Science and Technology (MAST) Center University of Colorado at Boulder 80309-0427, USA

<sup>b</sup> Department of Civil, Environmental and Architectural Engineering,

Membrane Applied Science and Technology (MAST) Center University of Colorado at Boulder 80309-0427, USA

<sup>c</sup> Department of Mechanical Engineering, University of Maine, Orono, 04473-5711, USA

Received 10 August 2006; received in revised form 8 October 2006; accepted 8 October 2006

Available online 4 December 2006

## Abstract

Biofilm growth on polymeric surfaces was monitored using ultrasonic frequency-domain reflectometry (UFDR). The materials utilized for this study included nonporous polycarbonate (PC) sheets, polyamide (PA) nanofiltration composite membranes and porous polyvinylidene fluoride (PVDF) microfiltration membranes (nominal pore size: 0.65  $\mu\text{m}$ ). Coupons of each material were placed in a biologically active annular reactor for up to 300 days, and subjected to a constant shear field (0.12  $\text{N m}^{-2}$ ), which induced sessile microbial growth from acetate amended municipal tap water. Acoustic monitoring was non-destructively executed by traversing coupons in a constant temperature water bath using a spherically focused 20-MHz immersion transducer. This semi-automated system was configured to obtain reflections from 50 regions (c.a.  $120 \times 10^3 \mu\text{m}^2$ ) distributed evenly near the centerline of each coupon. The resulting reflected power distributions were compared with standard biochemical and microscopic assays that described surface associated biofilms. When compared to clean (virgin) conditions, biofilms growing on coupons induced consistent attenuations in reflection amplitude, which caused statistically significant shifts in reflected power ( $p < 0.01$ ). Using exocellular polysaccharides as a surrogate measure of total biofilm mass, UFDR was able to detect biofilms developing on any of the materials tested at surface-averaged masses  $\leq 150 \mu\text{g cm}^{-2}$ . Above these threshold levels, increasing amounts of exocellular polysaccharides correlated with significant decreases in total reflected power (TRP). The distribution of biomass on the coupon surfaces determined by acoustic spectra was consistent with that observed using environmental scanning electron microscopy (ESEM). These results suggest that UFDR may be used as a non-destructive tool to monitor biofouling in a wide variety of applications.

© 2006 Published by Elsevier B.V.

**Keywords:** Biofilm; Ultrasonic reflectometry; Polysaccharides; Polymers; Biofouling

## 1. Introduction

In both natural and engineered systems, many microorganisms exist attached to surfaces associated with biofilms that grow in relatively oligotrophic environments (Costerton, 1999). In many situations, biofilms are undesirable artifacts of bacterial attachment: these heterogeneous films can often pose a (dangerous) nuisance in many environments, including industrial, and medical applications because they can provide microorganisms with significant resistance to biocides, anti-

biotics, and disinfectants, as well as promote undesirable genetic transfers (Costerton et al., 1987; Characklis and Cooskey, 1983; Roberson and Firestone, 1993; Bryers, 1993). Biofilms support pathogenic organisms in drinking water distribution systems, the lungs of cystic fibrosis patients, infections caused by medical implants, dental caries, contact lenses, and induce serious productivity losses in heat exchangers and filtration processes (Characklis and Cooskey, 1983; Ridgway and Flemming, 1996; Pasmore, 1999; Percival et al., 2000).

In many environments, bacterial cells suspended in solution will associate with a surface and reproduce; some cells excrete exocellular polysaccharides (EPS), which enable a conglomerate of cells to form substantial sessile communities. Biofilms are comprised of a complex hydrated milieu of microorganisms, void spaces, excreted byproducts, organic matter, particles,

\* Corresponding author. Department of Mechanical Engineering, University of Colorado at Boulder, 1111 Engineering Drive, 427 UCB, Boulder, CO 80309-0427, United States. Tel.: +1 303 492 5911; fax: +1 303 492 7317.

E-mail address: [mark.hernandez@colorado.edu](mailto:mark.hernandez@colorado.edu) (M. Hernandez).

precipitates, sorbed ions, organic molecules (Flemming et al., 1997; Sutherland, 2001), where water accounts for the majority of biofilm mass, often surpassing 90% of the total biomass (Schaule et al., 2000; Flemming et al., 1997; Sutherland, 2001). EPS, however, often comprises more than 90% of the dry weight of biofilms. It is difficult to categorize the exact state and location of biofilms due to their chaotic life cycles. In addition to their complex, heterogeneous composition, biofilms are also dynamic hydrogels which capriciously move, detach and reform on a wide variety of environmental or engineered surfaces (Hall-Stoodley et al., 2004); thus, real-time monitoring is required to accurately document the behavior of biofilms.

Conventional (and emerging) biofilm detection methods typically require destructive autopsies of both biofilm and substrates; however, acoustic techniques have the potential to monitor surface biofouling phenomena in real-time. Indeed, ultrasonic testing has been shown to effectively monitor the formation and growth of various foulants including calcium sulfate, protein and some microbiological communities (Mairal et al., 1999; Mairal et al., 2000; Sanderson et al., 2002; Li et al., 2002a, 2003; Li and Sanderson, 2002; Li et al., 2002b,c; Greenberg and Krantz, 2003; Zhang et al., 2003; Chai et al., in press) These studies suggest that ultrasonic *time-domain* reflectometry (UTDR) may be a desirable technique for the study of biofilm growth because of its *in-situ* reporting abilities.

Indeed, detecting the earliest stages of biofilm formation is critical to the efficient and cost-effective protection of many industrial and medical systems, and real-time biofilm monitoring could be used to initiate appropriate counter measures against biofilm maturation and help avoid detrimental effects associated with their attachments. We present a novel extension of UTDR signal processing into more sensitive ultrasonic *frequency-domain* spectra (UFDR), for the express purpose of biofilm surveillance. We report here that UFDR was capable of detecting early stages of biofilm growth as judged by standard biochemical EPS assays and direct microscopy. These results suggest that UFDR can be an effective real-time tool to monitor the maturation and detachment of biofilms from solid substrates of widely differing densities. The methodology is sufficiently general to enable its application to other systems of interest including water treatment membranes and pharmaceuticals separations processes.

## 2. Materials and methods

This investigation was executed in two phases. The first phase immobilized a spherically focused 20-MHz broadband transducer over a single point on a polycarbonate (PC) coupon subject to sessile microbiological growth of a pure bacterial culture. Acoustic reflections from the same micro-region (c.a. circular area c.a.  $120 \times 10^3 \mu\text{m}^2$ ) were observed over a six-week period. The second phase used a scanning paradigm, which was carried out by compiling acoustic reflection spectra from at least 150 different micro-regions on coupons sectioned from the PC sheets and the polyamide (PA) and polyvinylidene fluoride (PVDF) membranes, while multi-species biofilms enriched from a municipal drinking water, matured on their surfaces.

### 2.1. Pure-Culture biofilm induction for single point observations on polycarbonate coupons

For a subset of single point observations, the microorganisms used to produce a model biofilm were *Pseudomonas aeruginosa* (American Type Culture Collection, ATCC# 39324), which has been induced to produce copious amounts of exocellular polysaccharides in many studies. Cultures were grown overnight in a 250-mL batch reactor containing  $1 \text{ g L}^{-1}$  of tryptic soy broth (TSB). This inoculum was then transferred into a sterilized, 1-L annular biofilm reactor specifically designed to select and host sessile bacterial communities (BioSurface Technologies, Bozeman, MT). Two concentric cylinders composed the internal structure of the water-tight annular reactor. The outer cylinder was stationary and enclosed the entire system. The inner cylinder rotated at 20 rpm and contained 20 empty, beveled slots specifically manufactured to hold prefabricated  $15 \text{ cm} \times 1.5 \text{ cm}$  PC coupons. The reactor maintained continuous mixed and controlled at the shear rates of c.a.  $0.12 \text{ N m}^{-2}$ . The reactor was operated in a batch mode until biofilm began forming on the PC slides; this usually occurred within eight hours of operation. Following this inoculation period, the reactor was continuously fed with a sterile  $100\text{-mg TSB L}^{-1}$  solution, during which the hydraulic residence time was maintained at two hours.

### 2.2. Membrane coupon preparation

Experimental analysis was conducted on PA XLE nanofiltration (NF) membranes (Dow-FilmTEC; Minneapolis, MN) and PVDF Durapore™ microfiltration (MF) membranes (Millipore, Bedford, MA). The NF membranes have a composite structure with a thin, dense polyamide layer atop a thicker porous polyethersulfone support whereas the MF membranes are fully porous with nominal mean pore size of  $0.65 \mu\text{m}$ . Strips ( $20 \text{ cm} \times 12 \text{ cm}$ ) were cut from commercial membrane rolls and placed into a sterile container of a 70% isopropanol (Sigma-Aldrich, St. Louis, MO) purified using a  $0.22 \mu\text{m}$  vacuum filter (Nalgene, Rochester, NY) for 10 min. Subsequently, the membrane coupons were rinsed, and placed into a clean container of sterile-filtered deionized water for at least 2 h to ensure pores were free from residual alcohol. Following the setting procedure, coupons were cut into strips of approximately  $15 \text{ cm} \times 1.5 \text{ cm}$ . These strips were secured between a sterilized PC support and a sterilized stainless steel mask, and set with 1.5 mm screws. The PC and steel supports were autoclaved ( $121 \text{ }^\circ\text{C}$ , 2 atm) for 20 min prior to contact with membrane coupons. The mask contained windows with  $6 \text{ cm} \times 0.64 \text{ cm}$  dimensions, thus creating two windows for unobstructed acoustic analysis.

### 2.3. Biofilm induction on PC, PA and PVDF coupons

Biofouling studies on coupons were also conducted with the aid of a bench-scale annular reactor. Subsequent to the operations described for pure-culture, a naturally occurring bacterial consortium, which formed copious biofilms, was

enriched from unsterilized municipal tap water (Boulder, CO) amended with  $30 \text{ mg L}^{-1}$  of sodium acetate. This level of acetate was chosen in order to maintain an excess of readily assimilable carbon (C:N:P ratio 100:10:1 on a COD basis) for the express purpose of enriching a sessile bacterial population. The coupons were continuously exposed to an enrichment of microorganisms which proliferated inside the annular bioreactor. Pump, feed and motor controls were set at values that resulted in rapid sessile biological growth (1-day hydraulic residence time;  $0.12 \text{ N m}^{-2}$  shear rate), which ran uninterrupted up to 300 days. Under the specific operating parameters of this study, laminar flow conditions were maintained within the bioreactor ( $Re=267$ ). The bioreactor was wrapped in aluminum foil to reduce light exposure, photochemical reactions, and inhibit growth of photosynthetic organisms.

#### 2.4. Acoustic microscopy apparatus

An acoustic microscope, equipped with an ultrasonic pulser/receiver (Panametrics PR5052, Waltham MA), a 3.2-cm spherically focused broadband 20-MHz ultrasonic immersion transducer in a 0.6-cm diameter element (Panametrics V317, Waltham MA), and a digital storage oscilloscope (LeCroy 9350AM) was used to monitor biofilm development on the

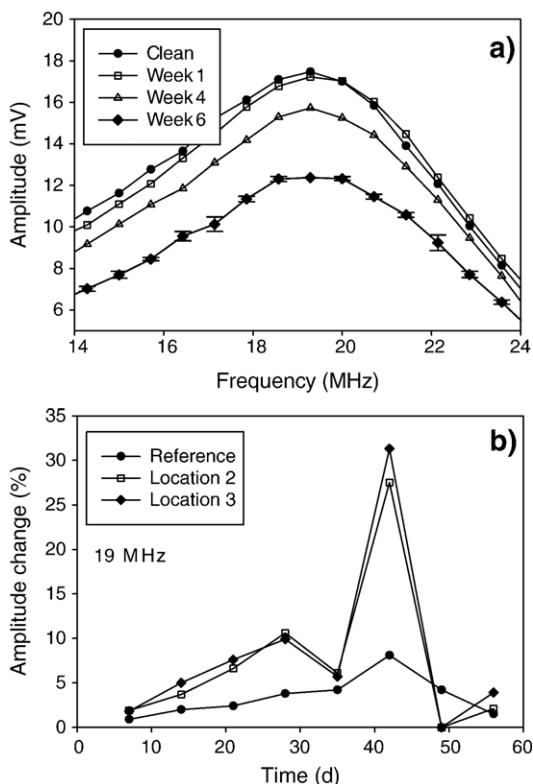


Fig. 1. Amplitude of sound waves reflected from a single point ( $120 \times 10^{-3} \mu\text{m}^2$ ) on polycarbonate coupons over a six-week period. Polycarbonate coupons were immersed in an annular reactor inducing the growth of *Pseudomonas aeruginosa* biofilms. Reflections were induced by a 20-MHz transducer: a) peak reflection amplitude in the range between 14 and 24 MHz; b) change in the amplitude (19 MHz) for two different locations with respect to a (clean) reference slide. The large amplitude change on day 49 corresponds with manual cleaning of the coupon surface.

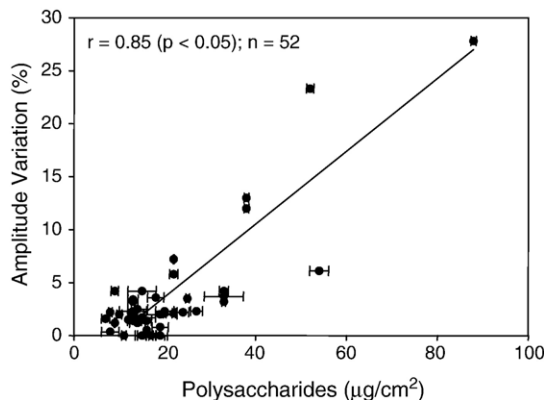


Fig. 2. Relationship between surface-associated polysaccharides and the amplitude variation of reflected acoustic signal from a single point on polycarbonate coupons (error bars represent one standard deviation;  $n=3$ ). Reflections (total sample size: 52) were induced by a 20-MHz transducer. Polycarbonate coupons were immersed in an annular bioreactor inducing the growth of *Pseudomonas aeruginosa* biofilms.

coupons. The apparatus was equipped with a micro-gear, 3-dimensional stage that enabled the transducer to be reproducibly positioned within  $\pm 50 \mu\text{m}$  of specified coordinates. For fixed-point observations of coupons hosting pure-culture *P. aeruginosa* biofilms, measurements were obtained by immersing slides in a sterile phosphate buffer ( $17.5 \text{ mgL}^{-1} \text{ KH}_2\text{PO}_4$  and  $7.5 \text{ mg L}^{-1} \text{ K}_2\text{HPO}_4$ ) maintained at  $16 \pm 1 \text{ }^\circ\text{C}$ . Each acoustic field (sampling area) was c.a.  $120 \times 10^3 \mu\text{m}^2$ . With each acoustic observation, the reflection time (ns), amplitude (V) and frequency (Hz) were recorded for the frequency range between 14 and 24 MHz.

A surface scanning mode was used to obtain areal distributions of acoustic reflections from coupons hosting multi-species biofilms. Using this mode, measurements were obtained by scanning slides immersed in filtered water maintained at  $30 \pm 1 \text{ }^\circ\text{C}$ , which propagates sound at  $1.503 \times 10^3 \text{ m s}^{-1}$ . Under this scanning paradigm, the transducer was programmed to traverse coupons in 1.14-mm linear increments, which generated reflections from at least 50 regions near the centerline of the coupon surfaces. Each coupon was traversed three times, for a total of 150 fields per each acoustic observation. With each acoustic observation, the reflection time (ns), amplitude (V) and frequency (Hz) were recorded for the frequency range between 5 and 30 MHz. Clean and fully saturated membrane coupons were analyzed acoustically prior to their insertion in the bioreactor. The resultant waveforms from all of the clean and fouled coupons for each of the three materials were compared against one another to demonstrate the acoustic reflection variability on different surfaces.

#### 2.5. Biochemical assay

Following acoustic characterization, each coupon was assayed for its polysaccharide content using modifications to the common Molisch test as reported by Daniels et al. (1994). To prevent undesired losses of biological material from the membranes surfaces, the entire coupon sample was placed into 20 mL pyrex test tubes (Kimble Glass, Inc, Vineland, NJ) to

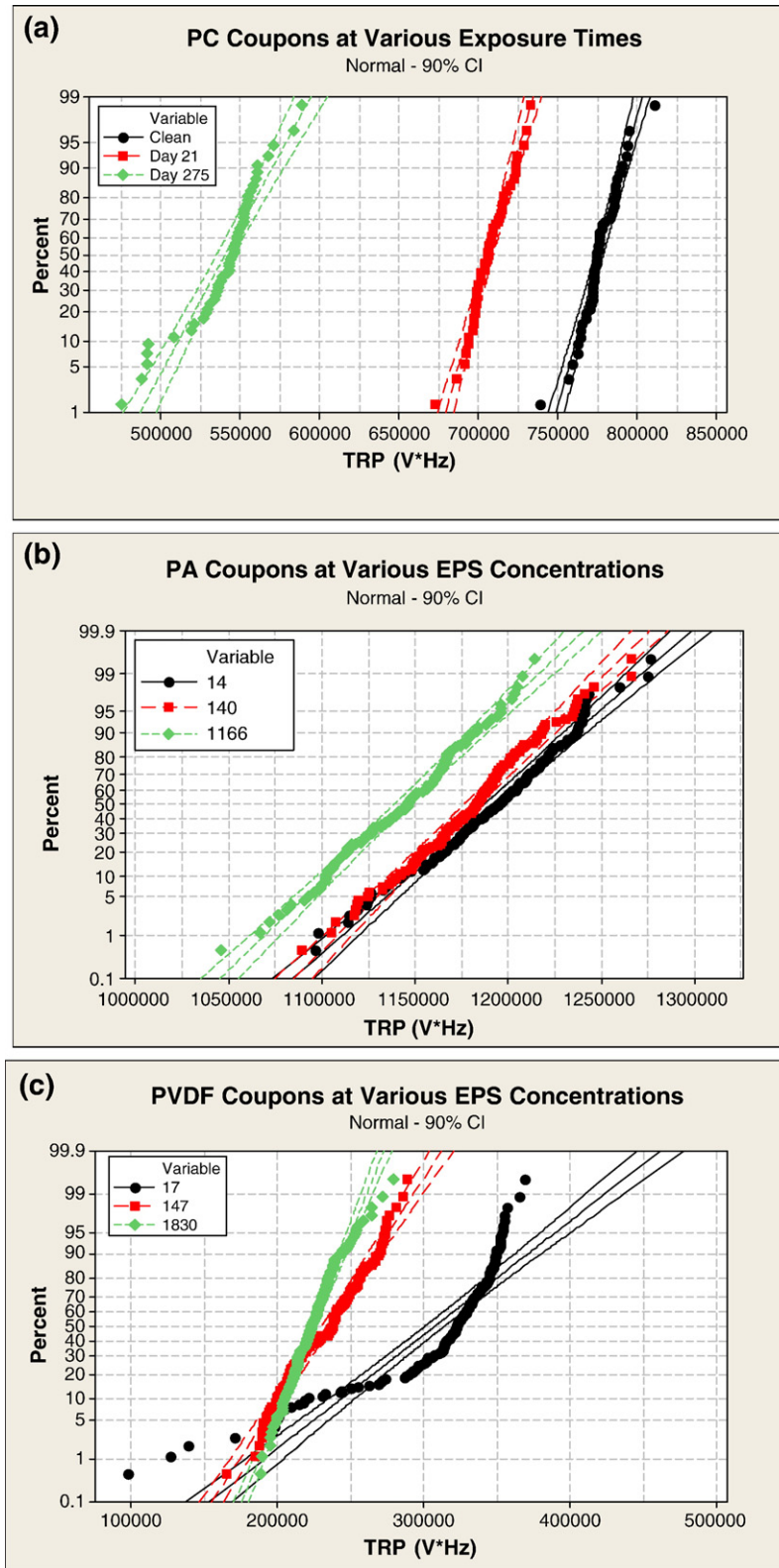


Fig. 3. Normality testing (90% confidence) of total reflected power from 150 acoustic observations from coupons hosting biofilm growth. Biofilm obtained using enriched tap water with different bioreactor exposure times, and results represent different biofilm accumulation on: a) polycarbonate, b) polyamide, and c) polyvinylidene fluoride coupons.

which 1.35 mL of phenol and 1.35 mL sterile deionized water was added. The solution was vortexed thoroughly for 1 min and was then placed into a sonicator containing ice water (Fisher Scientific, Fair Lawn, NJ) for 5 min. After mixing, 6.7 mL of

sulfuric acid (Mallinckrodt Baker, Inc., Paris, KY) was poured into each test tube and then vortexed for an additional 20 s. The solutions were left undisturbed at ambient temperature for 10 min followed by a constant, slow mixing for an additional

15 min. Approximately 2 mL of solution from each test tube was decanted into a cuvette (Fisher Scientific, Fair Lawn, NJ) at which time the absorbance readings of each sample were analyzed at 488 nm on an ultraviolet spectrophotometer (Hach DR/2010, Loveland, CO). Final absorbance results were compared to a serial dilution of dextrose standards (Mallinckrodt Baker Inc., Paris, KY) where the least-squared regression value exceeded 0.95. Standard EPA quality control procedures were used to determine the method detection limit, which was  $10 \mu\text{g mL}^{-1}$ . After the biochemical assay was completed, each coupon was rinsed with tap water to remove any remaining acid. Intact coupons were digitally scanned using a personal computer, commercial scanner (Hewlett Packard), and commercial software (SigmaScan, Leesburg, VA) to determine the effective exposure area of their surfaces. Prior to each measurement, the scan was calibrated with a ruler and each coupon area was measured.

### 2.6. Environmental scanning electron microscopy (ESEM) evaluation

Concurrent with biochemical analysis, samples of fouled coupons were isolated for ESEM evaluation. A cold ( $4^\circ\text{C}$ ) solution of potassium chloride (KCl) ( $40.89 \text{ mg}/150 \text{ mL}$  KCl; equinormal with acetate amended tap water) was used to store membrane coupons prior to ESEM analysis: membrane coupons were immersed in this sterile KCl solution for no more than 20 days prior to ESEM analysis.

### 2.7. Amplitude, frequency and total reflected power distributions

The reflection time and amplitude of reflected sound waves were recorded and compiled into frequency distributions with a Fourier transform using commercial software (Matlab, Mathworks, Inc., Natick MA) according to methods previously described by Ramaswamy (2002) and Ramaswamy et al. (2004). Regardless of sampling mode, the total reflected power (TRP) from each acoustic observation was determined by integrating the amplitude of reflected sound waves through the range of frequency observed. Frequency histograms were then compiled, tested for normality, and compared using widely accepted statistical indices (Levine et al., 2001) determined with commercial software (Minitab, SPSS Inc.).

### 2.8. Defined acoustic spectra

From every coupon scanned, 150 independent acoustic reflections were compiled into frequency spectra associated with 50 different sampling areas along the traverse of the coupons. Reflection amplitude was observed and recorded in the range between 5 and 30 MHz; this was determined as the most sensitive acoustic bandwidth with respect to biofilm growth on these polymeric surfaces. Total reflected power histograms were then ordered according to their associated EPS concentrations and normalized by their clean condition prior to biofilm development. Widely accepted statistical analyses were applied to test for normality and for significant differences between TRP distributions at different EPS levels.

### 2.9. Statistical analysis

Standard statistical analysis was applied to stringently assess differences and correlations between acoustic responses and EPS masses on different membrane materials. In this study, the Anderson–Darling normality test was applied to TRP data obtained from each membrane type; this test measures the deviation of a data set from a prescribed statistical distribution, resulting in a  $p$ -value. Smaller values of the Anderson–Darling coefficient correspond to an increasing probability that a given data set is normally distributed. The statistical standards in this study were established by choosing a 90% confidence level. As judged by Anderson–Darling, acoustic TRP spectra from PA and PC membranes could be fit with a normal distribution, thereby qualifying the application of parametric analyses of variance (ANOVA). Acoustic spectra from PVDF membranes were not normally distributed, requiring non-parametric statistical analyses. Analogous to a parametric ANOVA test, the Kruskal–Wallis test assesses significant differences between non-parametric distributions. The Kruskal–Wallis test is only suitable for independent, random samples with similar variances, but does not require symmetric data sets. Tukey's pairwise test at a 90% confidence level was used to evaluate if statistically significant shifts occurred in reflected power distributions when biofilms were developing on PC membranes.

## 3. Results

### 3.1. Single point observations

Acoustic response(s) to pure-culture biofilm formation was monitored at a single point on two different PC coupons for eight consecutive weeks. Fig. 1a shows the change in signal amplitude at the same location on slide surfaces during this period. Fig. 1b shows the percentage peak frequency (19 MHz) amplitude change for biofilm-fouled locations with respect to those same locations before they were introduced to the reactor (i.e. clean coupon). An otherwise identical coupon, which was never introduced into the reactor, was used as a reference to account for acoustic system variability during this sampling

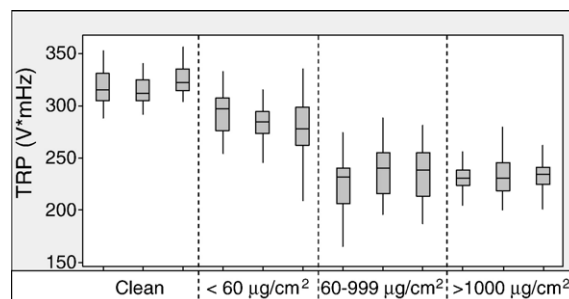


Fig. 4. Response of total reflected power during replicated scans of PVDF coupons hosting different polysaccharide masses which were grown from acetate amended tap water. Reflections were induced by a 20-MHz transducer. Each box represents 52 observations; vertical lines indicate minimum and maximum observations; upper and lower quartiles are represented by box boundaries; median values by central intersecting line.

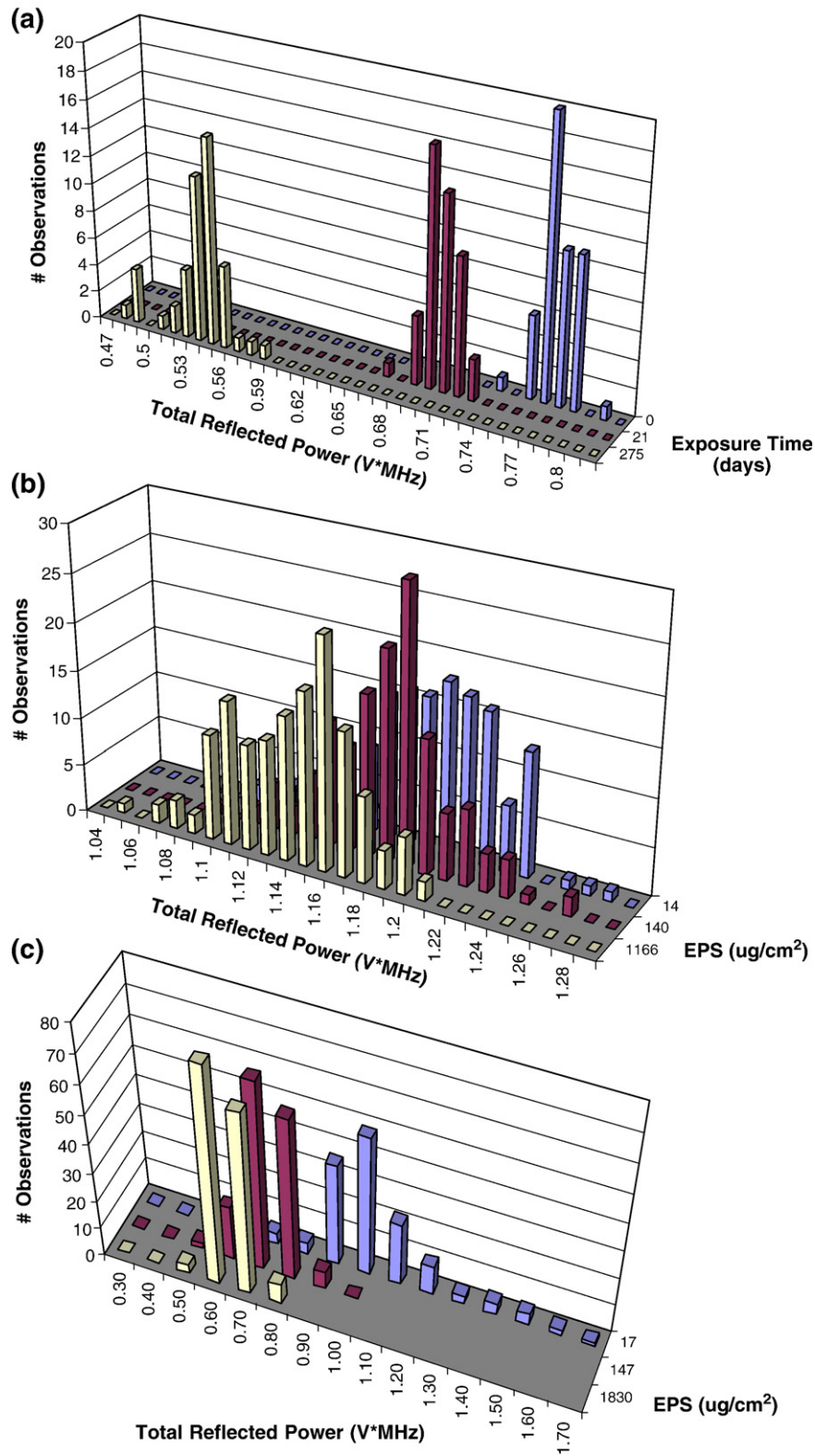


Fig. 5. Distributions of total reflection power showing reflected power reductions in response to increasing exposure time and EPS mass a) polycarbonate, b) polyamide and c) polyvinylidene fluoride coupons.

period. The amplitude change was defined as the decrease in signal amplitude due to the presence of biofilm, compared to the initial (clean coupon) amplitude. The large change in signal amplitude on day 49 corresponds with manual cleaning of the

coupon surface. Fig. 2 shows the relationship between the polysaccharide mass present on the PC coupon, and the corresponding changes in the reflection amplitude from the same isolated area on the coupon (c.a.  $120 \times 10^3 \mu\text{m}^2$ ).

### 3.2. Surface scanning observations

Over the course of ten months, PC, PA and PVDF coupons were systematically removed from annular bioreactor and evaluated for their acoustic and biochemical responses. An averaged TRP, expressed as  $V \times \text{MHz}$ , was the process variable isolated as responding to different degrees of biological growth. Fig. 3a (top) shows normality testing results where reflected power distributions from 150 points were compiled from PC coupons hosting varying masses of biofilm-associated polysaccharide. Similarly, the middle and bottom panels of Fig. 3b and c respectively show reflected power distributions and associated normality tests applied to 150 points on PA and PVDF membrane coupons with varying degrees of biofilm mass.

As judged by Anderson–Darling parametric analysis of reflected power distributions were normally distributed at a 90% confidence level when observed from PC and PA coupons. Tukey's pairwise test, also applied at a 90% confidence level, reported that statistically significant shifts in reflected power distributions occurred when biofilms developing on PC coupons exceeded  $35 \mu\text{g cm}^{-2}$ , and when surface-averaged polysaccharide masses exceeded  $140 \mu\text{g cm}^{-2}$  on PA membrane coupons.

However, acoustic TRP spectra observed from the PVDF membrane coupons were not normally distributed. A Kruskal–Wallis test was thus applied to assess significant differences between these non-parametric distributions where independent, random samples with similar variances were observed. The test statistic ( $H$ ) and its corresponding  $p$ -value delineated overall differences among the distributions at a confidence level of 95%. As judged by the Kruskal–Wallis test, the TRP distributions from microfiltration membrane coupons with a nominal pore size of  $0.65 \mu\text{m}$  were statistically different than its clean condition, yet statistical TRP similarities began to occur between membrane samples hosting biofilm growth at levels above  $60 \mu\text{g cm}^{-2}$  (Fig. 4). The relationship between reflection amplitude decline and biofilm EPS content was confirmed also with multiple point scanning observations when multi-species biofilms colonized PC, PA or PVDF coupons (Fig. 5).

### 3.3. ESEM evaluation

Fig. 6 presents electron microscopy images typical of clean and biofouled conditions of the PVDF membrane coupons observed. These images provided optical confirmation of the

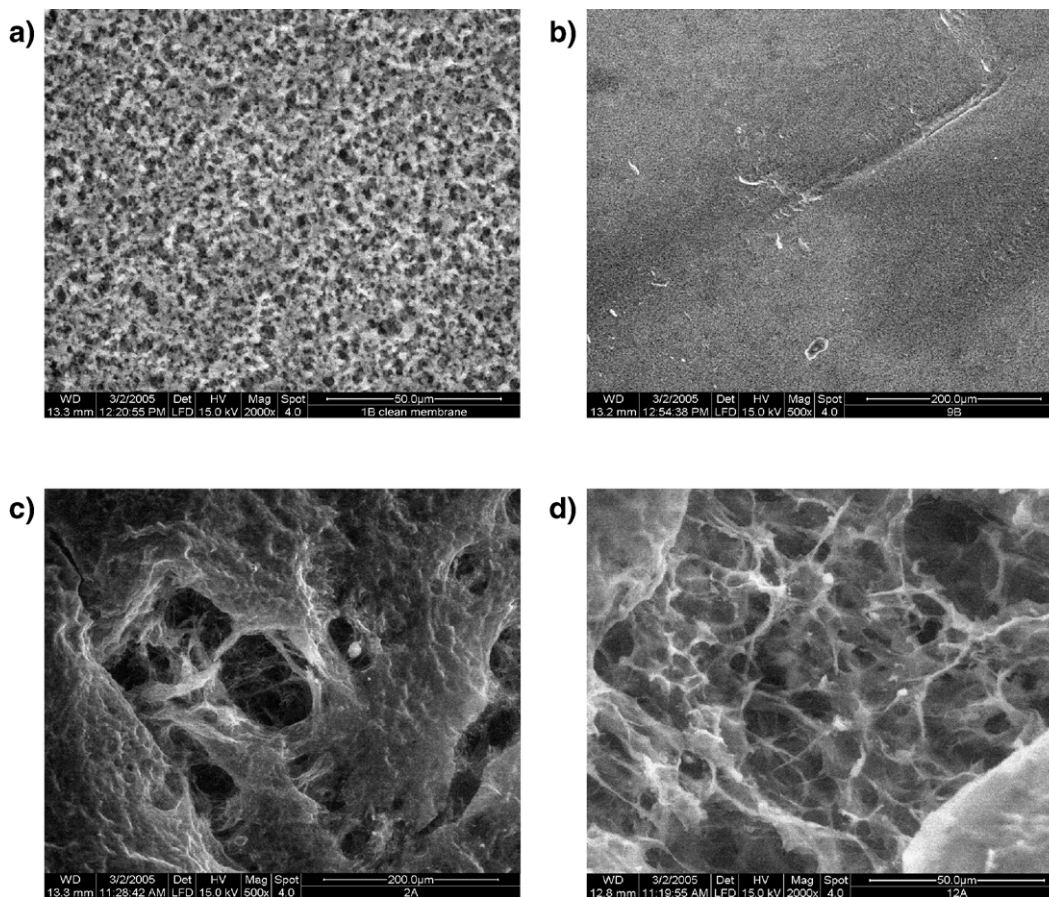


Fig. 6. ESEM images: a) a virgin PVDF membrane coupon surface ( $50 \mu\text{m}$  resolution,  $2000\times$  magnification); b) PVDF membrane coupon hosting a biofilm growth  $<100 \mu\text{g/cm}^2$  ( $200 \mu\text{m}$  resolution,  $500\times$  magnification); c) PVDF membrane coupon hosting a biofilm mass between  $101\text{--}999 \mu\text{g/cm}^2$  ( $200 \mu\text{m}$  resolution,  $500\times$  magnification). d) PVDF membrane coupon hosting a heavy biofilm growth, i.e.  $>1000 \mu\text{g/cm}^2$  ( $50 \mu\text{m}$  resolution,  $2000\times$  magnification).

discontinuous patchiness and continuous biomass, which respectively corresponded with early ( $<50 \mu\text{g cm}^{-2}$ ) and mature stages ( $>1000 \mu\text{g cm}^{-2}$ ) of biofilm development on the PVDF membrane coupons.

#### 4. Discussion

The intensity of the ultrasonic monitoring system used in this study, is comparable to the intensity of diagnostic ultrasonic systems used for many non-destructive medical applications. Typical allowable intensities in medical diagnostic ultrasound have a maximum near  $1.75 \text{ W cm}^{-2}$  with sufficient resolution, in cases such as fetal ultrasound, with intensity as low as  $100 \text{ mW cm}^{-2}$ . For comparative purposes, surgery is performed with ultrasonic systems that produce intensities on the order of  $1500 \text{ W cm}^{-2}$  (Harr, 2001). The intensity of the ultrasonic signal which insonified coupon associated biofilms in this study was dependent on the coupling efficiency at the biofilm interfaces. If the conversion efficiency is assumed to be 20% and the single interface from the housing to the feed is included, the intensity of the ultrasonic signal which insonifies the biofilm is approximately  $0.5 \text{ W cm}^{-2}$ . The intensity that was generated directly at the transducer face was within recommended non-destructive, medical diagnostic intensity levels, and the intensity at the biofilm interface was markedly lower because of attenuation in water. Such intensity levels are not expected to either result in mechanical damage or heating of the biofilm.

Our results confirmed that UFDR has sufficient sensitivity to detect biofilms growing on dense and porous polymeric surfaces, and suggest that this approach may be extended to biofilm monitoring on many different surfaces (and environments).

Related, but limited *time-domain* reflectometry studies have successfully used this non-destructive real-time approach to monitor organic and inorganic deposits on different polymeric surfaces. Li et al. (2003) successfully employed a *time-domain* approach to monitor fouling associated with paper mill effluent on polysulphone membranes in a cross-flow cell module. Mairal et al. (2000) demonstrated that relative amplitude changes of ultrasonic *time-domain* signals were indicative of the inception and maturation of an inorganic fouling layer on a reverse osmosis (RO) membrane. The amplitude values either increased or decreased with respect to a baseline waveform, depending on the extent of the fouling layer. In the study presented here, a clear trend emerged where amplitude changes and TRP values departures, calculated by *frequency-domain* transforms, were associated with microbial biofilm formation. Polysaccharides comprise between 75–95% of biofilm dry weight (Flemming et al., 1994), and were used herein as an effective mass surrogate to estimate biofilm association with the surface of (porous) polymers of widely differing density. Polysaccharides concentrations associated with biofilm growth in this study appear to be higher than those observed in other biofilm modeling studies. In bench-scale annual reactors that attempted to reproduce conditions in a drinking water distribution systems, the concentration of the carbohydrates in biofilm aged between 9 and 15 weeks were  $242 \pm 9 \text{ ng C cm}^{-2}$  and  $1069 \pm 211 \text{ ng C cm}^{-2}$ , respectively (Batte et al., 2003).

Deposit from a reverse osmosis membrane with the total weight of  $2.2 \text{ g m}^{-2}$  contained 7% of carbohydrate, which corresponded to a total carbohydrates concentration of  $15.4 \mu\text{g cm}^{-2}$  (Schaule et al., 2000).

Data presented here demonstrated a clear trend in reflection amplitude decline in response to increasing polysaccharide quantities on all coupons observed. The relationship between reflection amplitude decline and biofilm EPS content was confirmed under both single point and multiple point scanning observations: when *P. aeruginosa* biofilm was mechanically removed from PC coupon surfaces after six-weeks of growth, and the initial signal amplitude was restored (Fig. 1a and b), and when multi-species biofilms colonized PC, PA or PVDF coupons (Fig. 5). Fig. 2 summarizes the observed sensitivity of the UFDR method in a single point application; these results indicate that increasing amounts of biofilm-associated polysaccharide produce decreases in the corresponding signal reflection amplitude (Pearson correlation coefficient ( $r$ ) of 0.85;  $p < 0.05$ ).

Surface-normalized polysaccharide measurements ranged between 14 and  $1830 \mu\text{g cm}^{-2}$ . Frequency transformed acoustic reflectometry proved to be successful for detecting early stages of biofilm development, which is operationally defined here as surface polysaccharide concentrations in excess of  $35 \mu\text{g cm}^{-2}$ ; this threshold corresponded with the first acoustic reflection signals that were statistically different from reference signals on PC coupons. This threshold was significantly higher on PA or PVDF membrane coupons—on the order of  $150 \mu\text{g cm}^{-2}$ . This sensitivity difference is likely due to the lower acoustic impedance mismatch between the biofilm and the membranes, as well as the substantially greater porosity of the PVDF membrane coupons. The surface roughness, larger nominal pore size, as well as pore size distribution of the PVDF material may have contributed to the departure of normally distributed reflections observed from PVDF coupons, until biomass accumulated to levels high enough to dampen this effect (i.e. as tortuous pores filled with biopolymeric materials, a more homogenous acoustic surface was presented). Although the PVDF membrane has a pore size distribution in which the majority of the pores fall into the realm of the designated nominal pore size, many of the pores may be smaller or larger. The variability between pore sizes magnifies the chances of increased surface morphology differences and likely resulted in a less-consistent acoustic response.

At polysaccharide concentrations  $<35 \mu\text{g cm}^{-2}$ , a statistically significant relationship between polysaccharide and amplitude variation could not be established from single point observations. Since biofilms are heterogeneous structures of cell aggregates suspended in a polysaccharide matrix laden with water channels (Percival et al., 2000), it may be that at relatively low biofilm densities, and the surface-averaging of polysaccharide mass, could not appropriately account for variable and patchy coverage on a scale significantly less than the area of the acoustic sampling fields. The acoustic responses are sensitive to a local region of the reflecting surface, and a significant analytical artifact may be amplified by the differences in the areas sampled for biofilm polysaccharides and acoustic reflections, which were respectively  $2.4 \text{ cm}^2$  and  $\sim 120 \times 10^3 \mu\text{m}^2$  (scanning mode).

TRP median values decreased in response to increases in EPS concentration for PVDF membrane coupons with a nominal pore size of 0.65  $\mu\text{m}$ . The largest TRP departure occurred at the highest polysaccharide concentration (1830  $\mu\text{g cm}^{-2}$ ) with a 40% difference from the initial clean mean value. This suggests that biofouling contributes significantly to changing the surface roughness and/or bulk density of the membrane samples. At the various growth stages, the median TRP values were statistically different from one another, suggesting that real, inherent differences were detected by the acoustic technique.

Statistical evaluation suggests that TRP values decrease at relatively low EPS concentrations ( $<60 \mu\text{g cm}^{-2}$ ) on PVDF membranes (Fig. 4). Unlike the other materials tested, biological materials may enter the pores of the PVDF membranes, resulting in internal fouling. This phenomenon may occur simultaneously with biological deposition on the membrane surface, resulting in the combination of surface and internal fouling effects and may be responsible, in part or whole, for the non-normally distributed reflections observed from PVDF coupons. Since ultrasonic sensitivity relies on the impedance differences between overlapping interfaces, the acoustic response signal may be more sensitive in detecting density differences than surface roughness changes.

With respect to all the TRP distributions observed, departures were exhibited as biological growth progressed, yet, the degree of departure varied with substrate. This variability can likely be attributed to random and sporadic biological attachment at the earlier growth stages during which “patches” of microbial biomass covered the membrane surface; this was evident from ESEM characterizations of the membrane surfaces through the intermediate ranges of growth (Fig. 6). Under “patchy” conditions an acoustic signal may encounter growth or miss biofilm entirely, and reflect from the clean membrane surface just adjacent to a locally fouled region. Thus, patchy biofilm results in acoustic signals with high variability. Not until heavy growth accumulated was the appearance of biofilm patchiness and variability in TRP spectra reduced ( $>1000 \mu\text{g cm}^{-2}$ ).

## 5. Conclusions

Ultrasonic frequency-domain reflectometry was successfully employed here to detect biofilm development on three different substrates including dense polycarbonate, polyamide nanofiltration composite membranes, and fully porous polyvinylidene fluoride microfiltration membranes. A statistically significant correlation between the acoustic reflection characteristics and the extent of biofilm formation could be established when the biofilms contained more than 35  $\mu\text{g cm}^{-2}$  polysaccharides averaged over a PC coupon surface, and approximately 150  $\mu\text{g cm}^{-2}$  averaged over PA or PVDF coupon surfaces. Increasing amounts of exocellular polysaccharides, bound to the substrate surfaces, induced significant decreases in the reflection amplitude; these TRP reductions however, were not always proportional to the amounts of biofilm harvested from the coupon surfaces. Single point observations suggest the utility of a sentinel approach, which may be extended to monitoring operating separation modules (membrane treatment systems).

Overall, the UFDR methodology shows considerable promise as a useful tool for the study of biofilm development under a wide range of conditions.

## Acknowledgments

The authors wish to thank the NSF Industry/University Cooperative Research Center for Membrane Applied Science and Technology at the University of Colorado for research support, and to Rula Abu-Dalo, a research assistant who collaborated in the project during the Spring and Summer of 2001. In addition, A. Cristina Fonseca would like to thank the Fundação para Ciência e Tecnologia-Ministério da Ciência e Tecnologia.

## References

- Batte, M., Koudjonou, B., Laurent, P., Mathieu, L., Coallier, J., Prevost, M., 2003. Biofilm responses to aging and to high phosphate load in a bench-scale drinking water system. *Water Research* 37, 1351–1361.
- Bryers, J.D., 1993. Bacterial biofilms. *Current Opinion in Biotechnology* 4, 197–204.
- Chai, G.-Y., Greenberg, A.R., Krantz, W.B., 2007. Ultrasound, gravimetric, and SEM studies of inorganic fouling in spiral-wound membrane modules. *Desalination*, 208, 277–293.
- Characklis, W.G., Cooskey, K.E., 1983. Biofilms and microbial fouling. *Advances in Applied Microbiology* 29, 93–138.
- Costerton, J.W., 1999. The role of bacterial exopolysaccharides in nature and disease. *Journal of Industrial Microbiology and Biotechnology* 22, 551–563.
- Costerton, J.W., Irvin, R.T., Cheng, K.J., 1987. Bacterial biofilms in nature and disease. *Annual Review of Microbiology* 41, 435–464.
- Daniels, L., Hanson, R.S., Philips, J.A., 1994. Chemical analysis. In: Gerhardt, P., Murray, R.G.E., Wood, W.A., Krieg, N.R. (Eds.), *Methods for General and Molecular Bacteriology*. American Society for Microbiology, Washington, DC, pp. 512–554.
- Flemming, H.-C., Schaule, G., McDonogh, R., Ridgway, H.F., 1994. Effects and extent of biofilm accumulation in membrane systems. In: Geesey, G.G., Lewandowsky, Z., Flemming, H.-C. (Eds.), *Biofouling and Biocorrosion in Industrial Water Systems*. CRC Press/Lewis Publishers, Boca Raton, FL.
- Flemming, H., Schaule, G., Griebe, T., Schmitt, J., Tamachkiorowa, A., 1997. Biofouling—the Achilles heel of membrane processes. *Desalination* 113, 215–225.
- Greenberg, A.R., Krantz, W.B., 2003. Ultrasonic sensors for the real-time measurement of reverse osmosis membrane module fouling and cleaning. *Fluid/Particle Separation Journal* 15, 43–49.
- Hall-Stoodley, L., Costerton, J.W., Stoodley, P., 2004. Bacterial biofilms: from the natural environment to infectious diseases. *Nature Reviews Microbiology* 2, 95–108.
- Harr, G., 2001. Acoustic surgery. *Physics Today* 54, 29–34.
- Levine, D.M., Ramsey, P.P., Smidt, R.K., 2001. *Applied Statistics for Engineers and Scientists*. Prentice Hall, Inc., Saddle River, NJ.
- Li, J., Sanderson, R.D., 2002. In situ measurement of particle deposition and its removal in microfiltration by ultrasonic time-domain reflectometry. *Desalination* 146, 169–175.
- Li, J., Hallbauer-Zadorozhnaya, V.Y., Hallbauer, D.K., Sanderson, R.D., 2002a. Cake-Layer Deposition, Growth, and Compressibility during Microfiltration Measured and Modeled Using a Non-invasive Ultrasonic Technique. *Industrial & Engineering Chemistry Research* 41, 4106–4115.
- Li, J., Sanderson, R.D., Hallbauer, D.K., Hallbauer-Zadorozhnaya, V.Y., 2002b. Measurement and modeling of organic fouling deposition in ultrafiltration by ultrasonic transfer signals and reflections. *Desalination* 146, 177–185.
- Li, J., Sanderson, R.D., Jacobs, E.P., 2002c. Non-invasive visualization of the fouling of microfiltration membranes by ultrasonic time-domain reflectometry. *Journal of Membrane Science* 201, 17–29.

- Li, J., Hallbauer, D.K., Sanderson, R.D., 2003. Direct monitoring of membrane fouling and cleaning during ultrafiltration using a non-invasive ultrasonic technique. *Journal of Membrane Science* 215, 33–52.
- Mairal, A.P., Greenberg, A.R., Krantz, W.B., Bond, L.J., 1999. Real-time measurement of inorganic fouling of RO desalination membranes using ultrasonic time-domain reflectometry. *Journal of Membrane Science* 159, 185–196.
- Mairal, A.P., Greenberg, A.R., Krantz, W.B., 2000. Investigation of membrane fouling and cleaning using ultrasonic time-domain reflectometry. *Desalination* 130, 45–60.
- Pasmore, M., 1999. Analysis and Prevention of Biofilm Fouling Initiation on Water Processing Membranes, PhD Thesis, Department of Chemical Engineering, University of Colorado at Boulder.
- Percival, S.L., James, T.W., Hunter, P.R., 2000. *Microbial Aspects of Biofilms and Drinking Water*. CRC Press LLC, Boca Raton, FL.
- Ramaswamy, S., 2002. Development of an ultrasonic technique for the non-invasive characterization of membrane morphology. In *Mechanical Engineering*, PhD thesis, p. 192. Boulder, CO: University of Colorado.
- Ramaswamy, S., Greenberg, A.R., Peterson, M.L., 2004. Non-invasive measurement of membrane morphology via UFDR: pore-size characterization. *Journal of Membrane Science* 239, 143–154.
- Ridgway, H., Flemming, H.-C., 1996. Membrane Biofouling in Water Treatment Membrane Processes. In: Mallevalle, J., Odendal, J., Wiesner, P.E. (Eds.), McGraw-Hill, Columbus, OH.
- Roberson, E.E., Firestone, M.K., 1993. Relationship between desiccation and exopolysaccharide production in a soil *Pseudomonas sp.* *Applied and Environmental Microbiology* 58, 1284–1291.
- Sanderson, R.D., Li, J., Koen, L.J., Lorenzen, L., 2002. Ultrasonic time-domain reflectometry as a non-destructive instrumental visualization technique to monitor inorganic fouling and cleaning on reverse osmosis membranes. *Journal of Membrane Science* 207, 105–117.
- Schaule, G., Griebel, T., Flemming, H.-C., 2000. Steps on biofilm sampling and characterization in biofouling cases. In: Flemming, H.-C., Szewzyk, U., Griebel, T. (Eds.), *Biofilms: Investigative Methods and Applications*. Technomic Publishing Company, Inc., Lancaster, Pennsylvania, pp. 1–21.
- Sutherland, I.W., 2001. Biofilm exopolysaccharides: a strong and sticky framework. *Microbiology* 147, 3–9.
- Zhang, Zh.-X., Greenberg, A.R., Krantz, W.B., Chai, G.-Y., 2003. Study of membrane fouling and cleaning in spiral wound modules using ultrasonic time-domain reflectometry. In: Butterfield, A.A., Bhattacharyya, D. (Eds.), *New Insights into Membrane Science and Technology: Polymeric, Inorganic and Biofunctional Membranes*. Elsevier, Amsterdam, pp. 65–88.